**Electronic Supplementary Information**

# Growth of $CoFe_2O_4$ hollow nanoparticles on graphene sheets for high-performance electromagnetic wave absorber

Feng Yan,[a] Shen Zhang,[a] Xiao Zhang,[a] Chunyan Li,[a] Chunling Zhu,*[b] Xitian Zhang,[c] and Yujin Chen*[a]

[a] Key Laboratory of In-Fiber Integrated Optics, Ministry of Education and College of Science, Harbin Engineering University, Harbin 150001, China.

[b] College of Chemistry and Chemical Engineering, Harbin Engineering University, Harbin 150001, China.

[c] Key Laboratory for Photonic and Electronic Bandgap Materials, Ministry of Education and School of Physics and Electronic Engineering, Harbin Normal University, Harbin 150025, China.

*Corresponding authors.
E-mail addresses: zhuchunling@hrbeu.edu.cn (C. Zhu) or chenyujin@hrbeu.edu.cn (Y. Chen).

## Experimental details

**Chemicals.** Graphene sheets were purchased from Nanjing XFNANO Material Tech Co., Ltd. (Nanjing City, China). Cobalt acetate, ferric acetylacetonate and ammonia were purchased from Tianjin Kermel Chemical Reagent Co., Ltd. (China). Commercially available chemical reagents were used without further purification.

**Synthesis of $CoFe_2O_4$-HNP/G.** Typically, 24 mg of graphene was dispersed in 72 mL of ethanol and sonicated for 20 min. Then 25 mg of cobalt acetate, 71 mg of ferric acetylacetonate were added. After ultrasonication sonication for another 15 min, 3.6 mL of distilled water and 2 mL of ammonia were added into the above solution, respectively. The mixture was sealed in a flask and kept at 80 °C for 10 h under magnetic stirring. After the reaction and cooling to room temperature, the precipitate (CoFe hydroxide/G) in the solution was collected and then washed with distilled water and absolute ethanol several times and dried through a freeze-drying process. In the next step, the CoFe alloy NPs/G was obtained after heating CoFe hydroxide/G in a furnace at 350°C for 3 h under an $H_2$/Ar flow. After that, the CoFe alloy NPs/G was treated in a tube furnace at 200℃ for 2 h and 280℃ for 2 h under air atmosphere to obtain the $NiCo_2O_4$-HNP/G.

**Synthesis of $CoFe_2O_4$-SNP/G $Co_3O_4$-SNP/G and $Fe_2O_3$-SNP/G.** Under the same conditions, $CoFe_2O_4$-SNP/G was obtained by directly heating the CoFe hydroxide/G in a tube furnace at 200 °C for 2 h and 280 °C for 2 h. $Co_3O_4$-SNP/G and $Fe_2O_3$-SNP/G were synthesized by directly adding cobalt acetate (75 mg) or ferric acetylacetonate (106 mg) only in the first step, and the corresponding precursor were heated in a tube

furnace at 200°C for 2 h and 280 °C for 2 h in air flow, respectively.

**Structure Characterizations.** XRD data were measured by a Rigaku D/max-2600/PC with Cu Kα radiation (λ=1.5418Å). The morphology and size of samples were characterized by scanning electron microscope (Hitachi SU70) and an FEI Tecnai-F20 transmission electron microscope equipped with a Gatan imaging filter (GIF). BET surface area and pore volume were tested with a Quantachrome Instruments NOVA4000 after the composites were vacuum dried at 200℃ over 10 h. XPS analyses were carried out by using a spectrometer with Mg Kα radiation (PHI 5700 ESCA System).The binding energy was calibrated with the C 1s position of contaminant carbon in the vacuum chamber of the XPS instrument (284.6 eV).

**Electromagnetic Parameters Measurements.** The composite (50 wt%) was uniformly mixing with a paraffin matrix and cut into toroidal shaped samples of 7.00 mm in outer diameter, 3.00 mm in inner diameter, and 3.00 mm in thickness. The measurement was recorded by using an Anritsu MS4644A Vectorstar vector network analyzer (VNA) with a sweep oscillator and a S-parameter test set in the frequency of 2 – 18 GHz. Before measurement the electromagnetic parameter, a full two-port calibration was verified by standard Teflon sample.

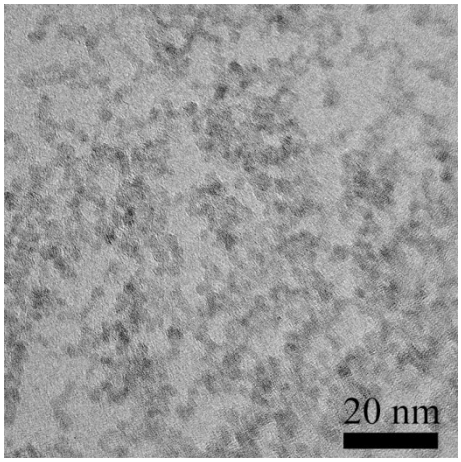


**Fig. S1** The low-magnification TEM image of CoFe hydroxide/G.

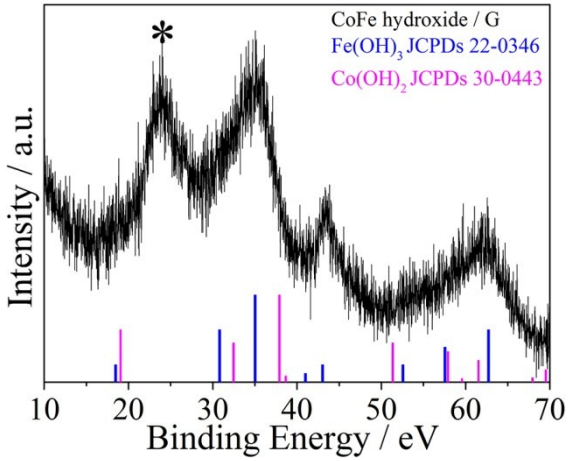


**Fig. S2.** The XRD pattern of CoFe hydroxide/G.

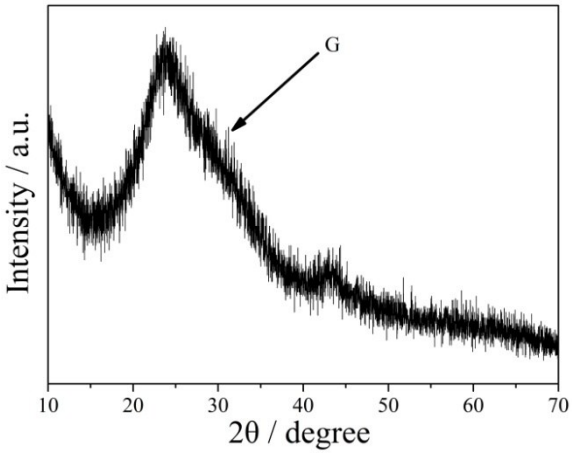


**Fig. S3.** The XRD pattern of pure graphene sheets.

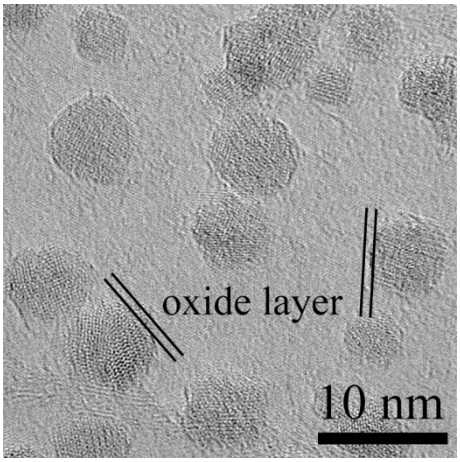


**Fig. S4** The high-magnification TEM image of CoFe alloy NPs/G.

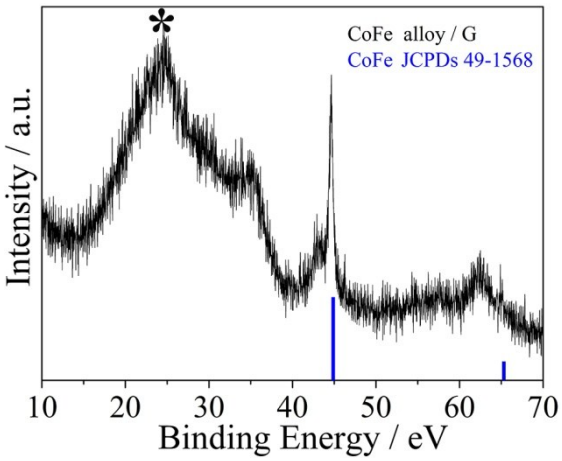


**Fig. S5.** The XRD pattern of CoFe alloy NPs/G.

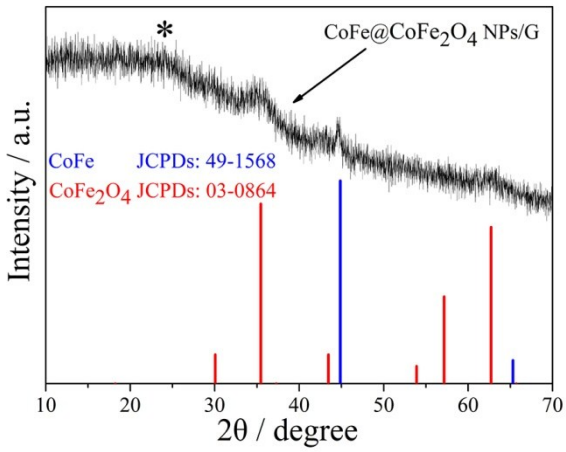


**Fig. S6.** The XRD pattern of $CoFe@CoFe_2O_4$ NPs/G.

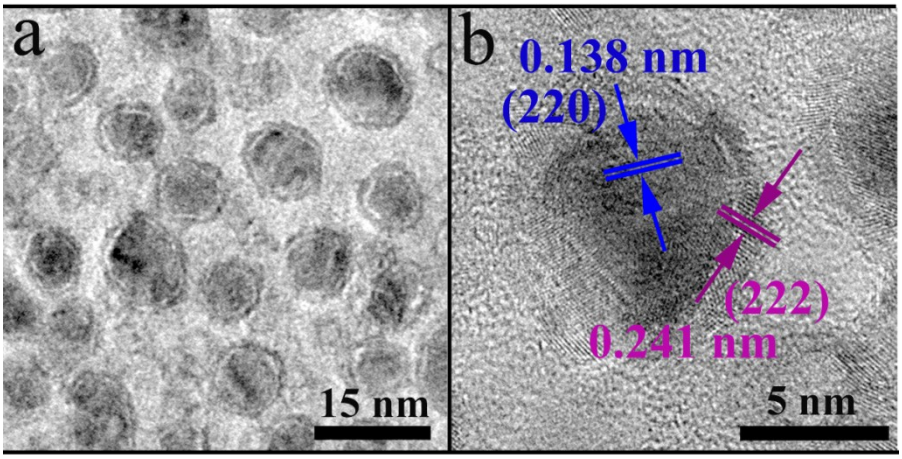


**Fig. S7.** a) Low-magnification TEM, b) HRTEM images of $CoFe@CoFe_2O_4$ NPs/G.

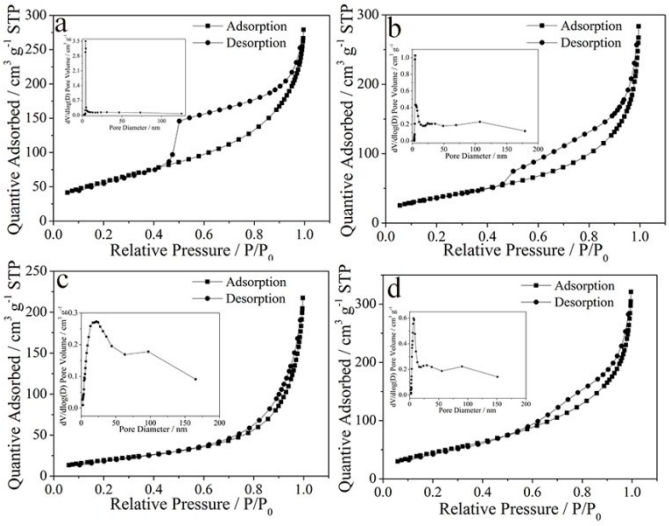


**Fig. S8.** Nitrogen adsorption and desorption isotherms of $CoFe_2O_4$-HNP/G a), $CoFe_2O_4$-SNP/G b), $Co_3O_4$-SNP/G c), and $Fe_2O_3$-SNP/G d). The insets of a-d) show the corresponding pore-size distribution calculated by the BJH method.

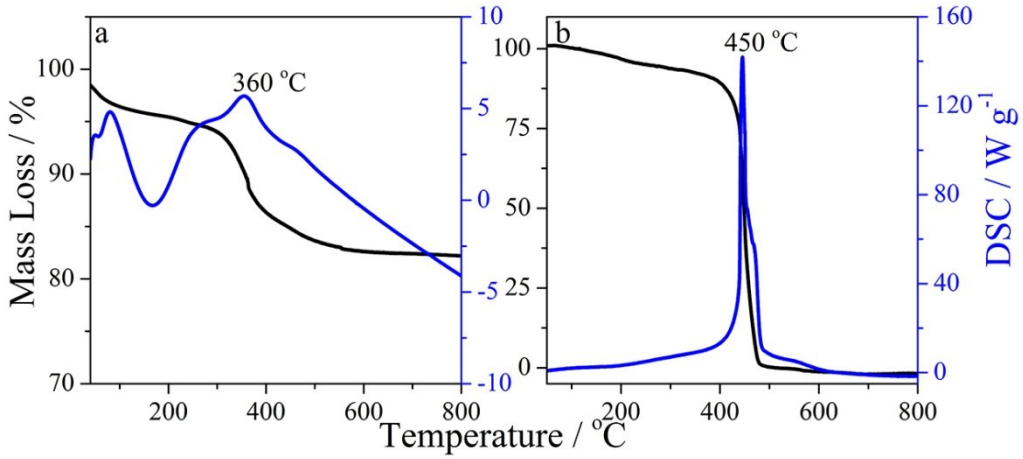


**Fig. S9.** The TGA and DSC patterns $CoFe_2O_4$-HNP/G a), and pristine graphene b).

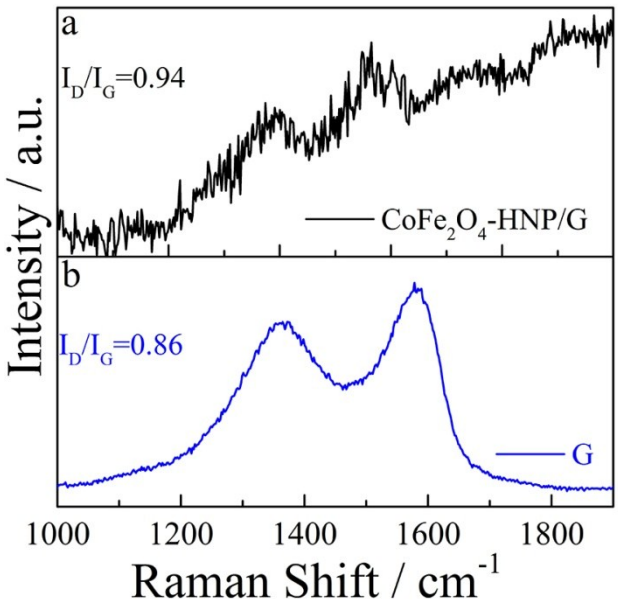


**Fig. S10.** The Raman spectrum of $CoFe_2O_4$-HNP/G a), and pristine graphene b).

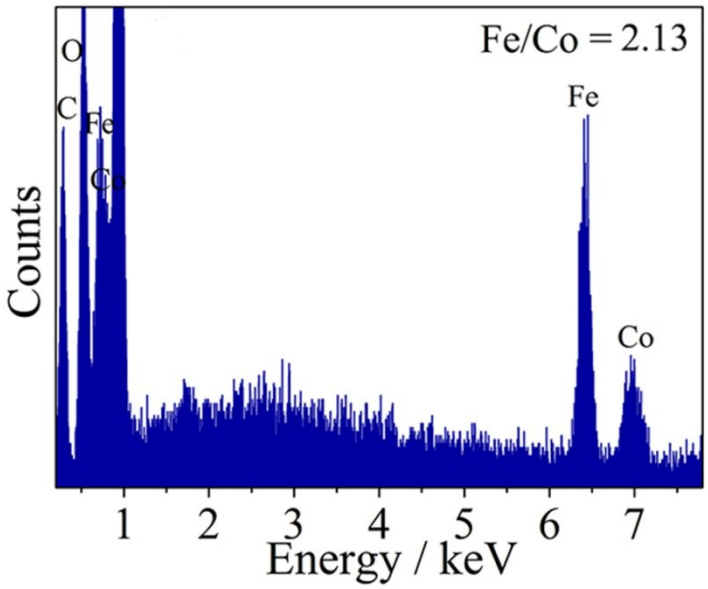


**Fig. S11.** The EDS patterns of $CoFe_2O_4$-HNP/G.

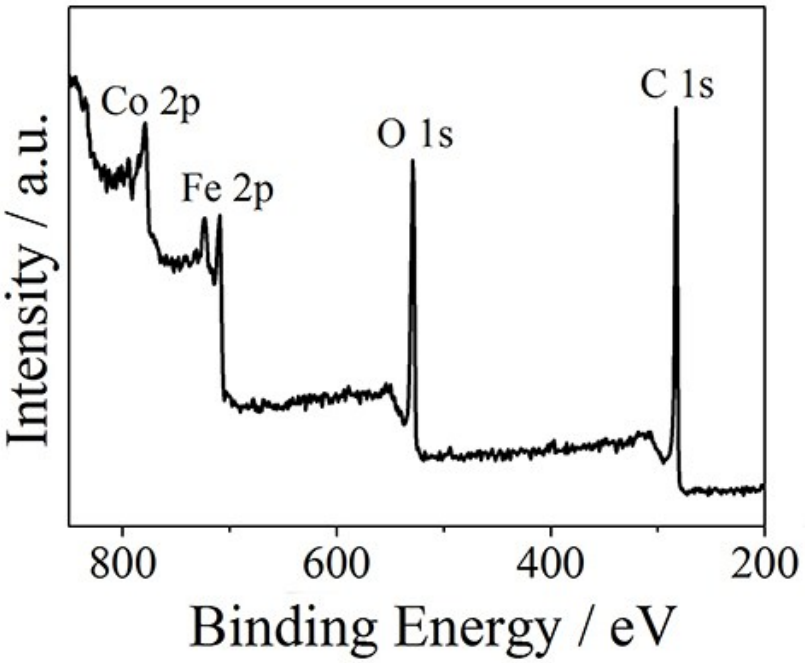


**Fig. S12.** The survey XPS spectrum of $CoFe_2O_4$-HNP/G.

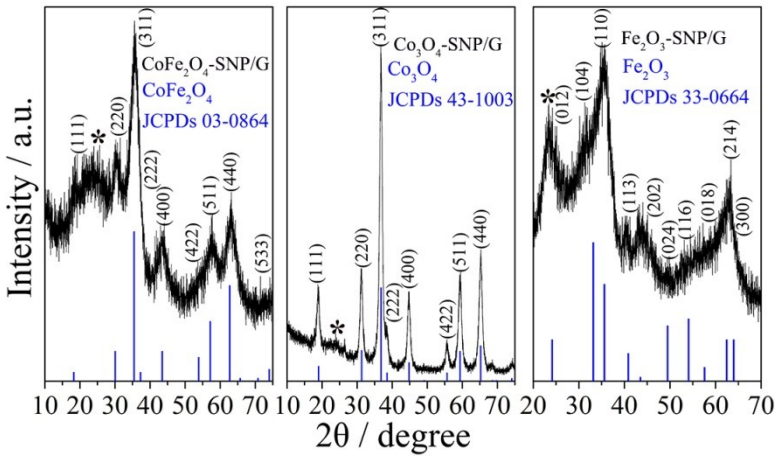


**Fig. S13.** The XRD patterns of $CoFe_2O_4$-SNP/G a), $Co_3O_4$-SNP/G b), and $Fe_2O_3$-SNP/G c).

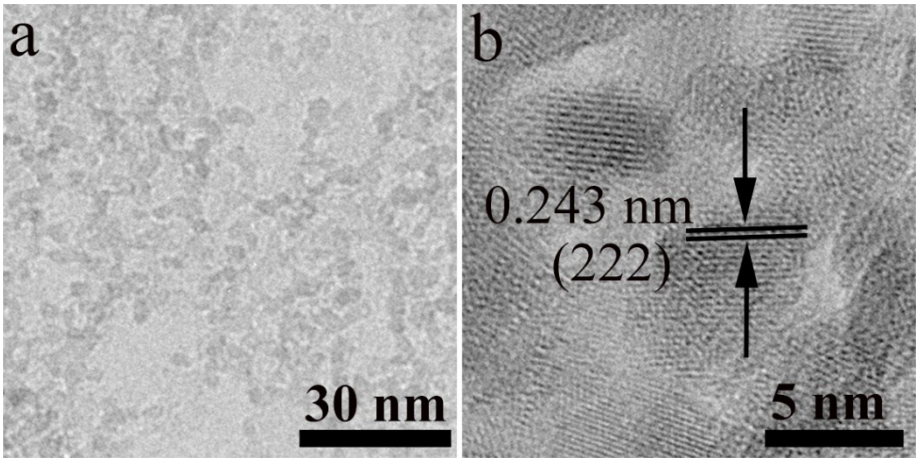


**Fig. S14.** The low-magnification TEM a), and HRTEM images of $CoFe_2O_4$-SNP/G b).

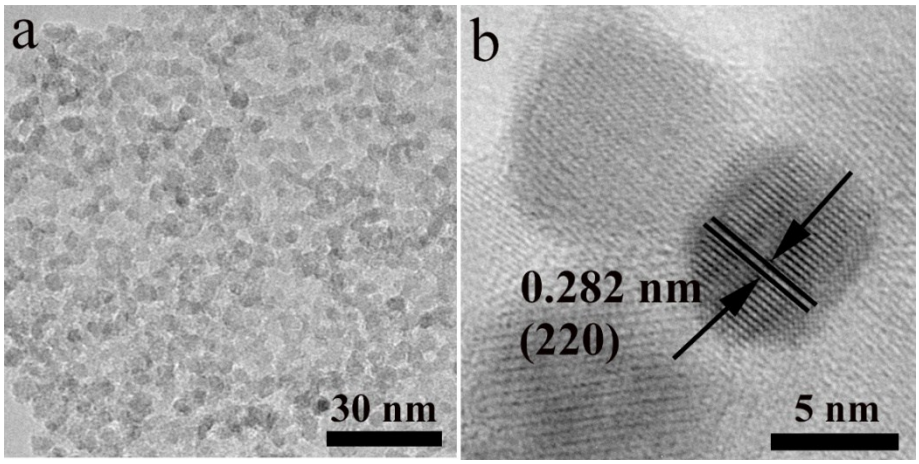


**Fig. S15.** The low-magnification TEM a), and HRTEM images of $Co_3O_4$-SNP/G b).

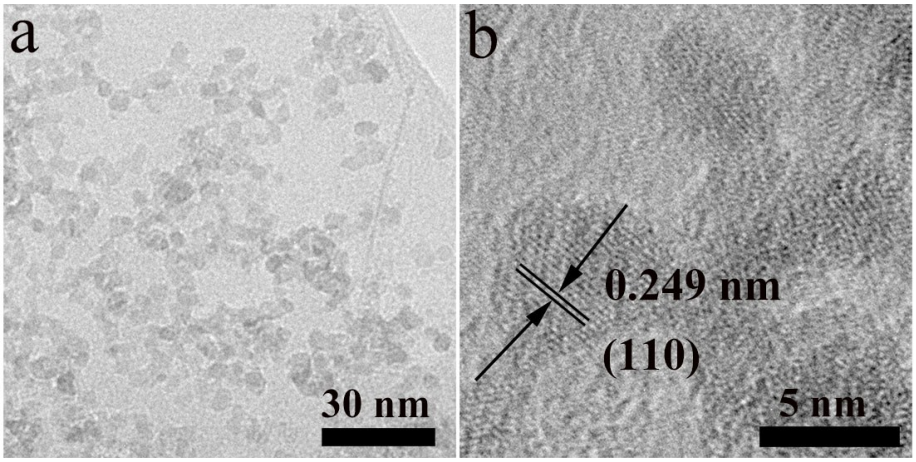


**Fig. S16.** The low-magnification TEM a), and HRTEM images of $Fe_2O_3$-SNP/G b).

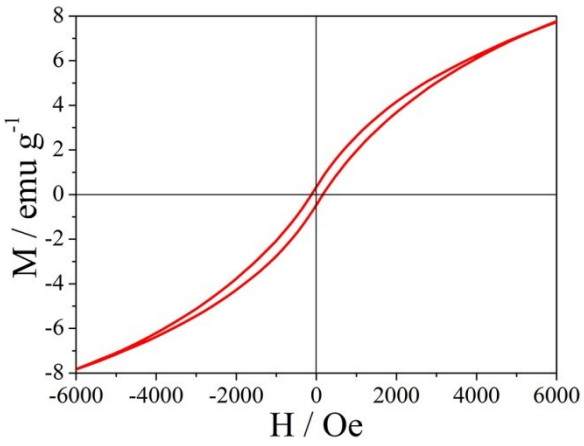


**Fig. S17.** Magnetization hysteresis loop of the $CoFe_2O_4$-HNP/G.

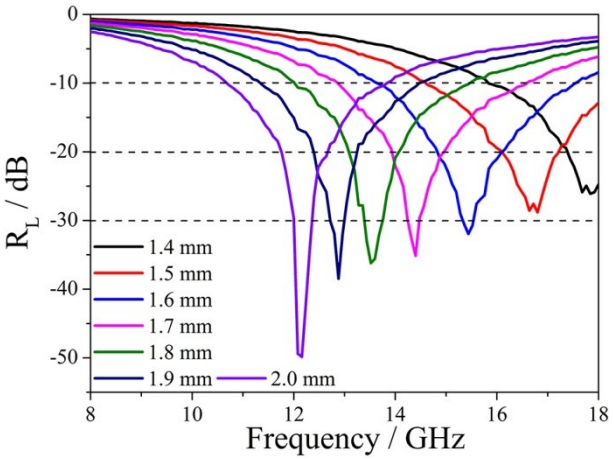


**Fig. S18.** The calculated $R_L$–$f$ curves of $CoFe_2O_4$-HNP/G at the absorber thickness ranging from 1.4 – 2.0 mm.

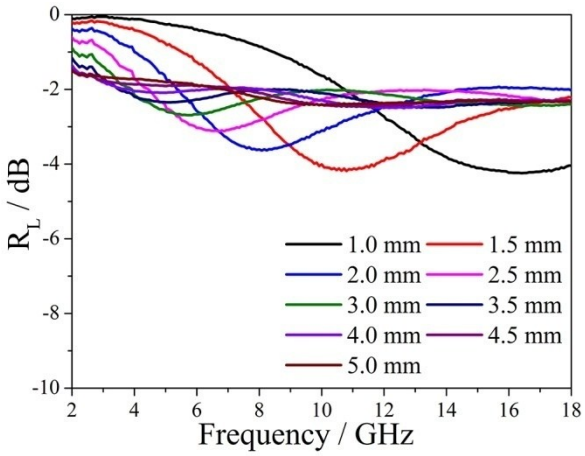


**Fig. S19.** The calculated $R_L$–$f$ curves of pure graphene sheets at different thicknesses in the frequency of 2 – 18 GHz.

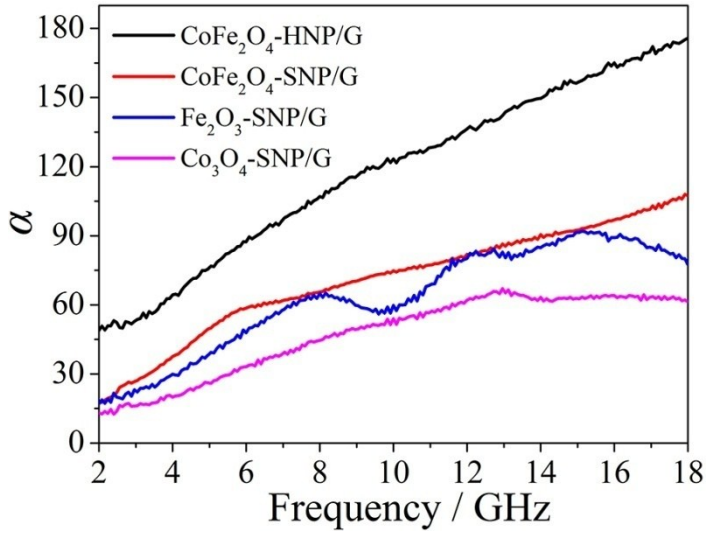


**Fig. S20.** The attenuation constants of $CoFe_2O_4$-HNP/G, $CoFe_2O_4$-SNP/G, $Fe_2O_3$-SNP/G and $Co_3O_4$-SNP/G over 2 – 18 GHz.

**Table S1.** The mass ratio of C, O, Fe, and Co is estimated from the survey spectra of XPS.

| Element | Mass ratio (%) |
|---|---|
| **Fe** | 34.26 |
| **Co** | 18.05 |
| **O** | 28.65 |
| **C** | 19.04 |

**Table S2.** Comparison of EMW absorption properties of $CoFe_2O_4$-HNP/G with other reported absorbing materials.

| Materials | Minimal $R_L$ (dB) | $d$ (mm) | EAB (GHz) | C (wt %) | Ref. |
|---|---|---|---|---|---|
| $CoFe_2O_4$ | –34.1 | 2.5 | 2.6 | 50 | [1] |
| PANI/$CoFe_2O_4$/PVDF | –57.7 | 4.0 | 3.4 | – | [2] |
| $CoFe_2O_4$/graphene | –36.4 | 2.5 | ~5.2 | 70 | [3] |
| $CoFe_2O_4$/graphene | –24.7 | 4.0 | ~2.4 | 60 | [4] |
| $CoFe_2O_4$/reduced graphene oxide | –57.7 | 2.8 | 5.8 | 50 | [5] |
| $NiFe_2O_4$-polystyrene | –13.0 | 2.0 | 2.7 | 65 | [6] |
| FeCo/graphene | –40.2 | 2.5 | ~4.1 | 50 | [7] |
| C@$NiCo_2O_4$@$Fe_3O_4$ | –43 | 3.4 | 2.1 | 60 | [8] |
| RGO/$NiFe_2O_4$ | –39.7 | 3.0 | ~3.0 | 50 | [9] |
| Porous Co/C | –35.3 | 4.0 | ~2.4 | 40 | [10] |
| CoNi–C | –50.2 | 4.0 | ~3.4 | 50 | [11] |
| $Fe_3O_4$ | –28.3 | 2.0 | ~3.5 | 50 | [12] |
| $Co_3O_4$-SNP/G | –8.9 | 4.0 | – | 50 | This work |
| $Fe_2O_3$-SNP/G | –16.2 | 4.5 | 2.0 | 50 | This work |
| $CoFe_2O_4$-SNP/G | –20.6 | 4.5 | 1.5 | 50 | This work |
| $CoFe_2O_4$-HNP/G | –50.2 | 2.0 | 3.2 | 50 | This work |

## REFERENCES


1. Zhang, S. L.; Jiao, Q. Z.; Zhao, Y.; Li, H. S.; Wu, Q. Preparation of Rugby-shaped $CoFe_2O_4$ Particles and their Microwave Absorbing Properties. *J. Mater. Chem. A,* 2014, **2**, 18033–18039.
2. Yang, H. B.; Han, N.; Lin, Y.; Zhang, G.; Wang, L. Enhanced Microwave Absorbing Properties of PANI/$CoFe_2O_4$/PVDF Composite. *RSC Adv.,* 2016, **6**, 100585–100589.

3. Li, X. H.; Feng, J.; Zhu, H.; Qu, C. H.; Bai, J. T.; Zheng, X. L. Sandwich-like Graphene Nanosheets Decorated with Superparamagnetic $CoFe_2O_4$ Nanocrystals and their Application as an Enhanced Electromagnetic Wave Absorber. *RSC Adv.,* 2014*,* **4***,* 33619–33625.
4. Fu, M.; Q. Jiao, Z.; Zhao, Y.; Li, H. S. Vapor Diffusion Synthesis of $CoFe_2O_4$ Hollow Sphere/Graphene Composites as Absorbing Materials. *J. Mater. Chem. A,* 2014, **2**, 735–744.
5. Liu, Y.; Chen, Z.; Zhang, Y.; Feng, R.; Chen, X.; Xiong, C. X.; Dong, L. J. Broadband and Lightweight Microwave Absorber Constructed by in Situ Growth of Hierarchical $CoFe_2O_4$/Reduced Graphene Oxide Porous Nanocomposites. *ACS Appl. Mater. Interfaces,* 2018*,* **10***,* 13860-13868.
6. Zhao, H. T.; Sun, X. D.; Mao, C. H.; Du, J. Preparation and Microwave–absorbing Properties of $NiFe_2O_4$-polystyrene Composites. *Physica B,* 2009, **404**, 69–72.
7. Li, X. H.; Feng, J.; Du, Y. P.; Bai, J. T.; Fan, H. M.; Zhang, H. L.; Peng, Y.; Li, F. S. One-pot Synthesis of $CoFe_2O_4$/Graphene Oxide Hybrids and Their Conversion into FeCo/graphene Mybrids for Lightweight and Highly Efficient Microwave Absorber. *J. Mater. Chem. A*, 2015, **3**, 5535–5546.
8. Wei ,S.; Wang, X. X.; Zhang, B. Q.; Yu, M. X.; Zheng, Y. W.; Wang, Y.; Liu J. Q.. Preparation of Hierarchical Core-shell C@$NiCo_2O_4$@$Fe_3O_4$ Composites for Enhanced Microwave Absorption Performance. *Chemical Engineering Journal,* 2017**,** **314***,* 477–487.
9. Zong, M.; Huang, Y.; Ding, X.; Zhang, N.; Qu, C. H.; Wang, Y. L.; One-step

Hydrothermal Synthesis and Microwave Electromagnetic Properties of RGO/$NiFe_2O_4$ Composite. *Ceramics International,* 2014**, 40**, 6821–6828.

10. Lü, Y. Y.; Wang, Y. T.; Li, H. L.; Lin, Y.; Jiang, Z. Y.; Xie, Z. X.; Kuang, Q.; Zheng, L. S. MOF-Derived Porous Co/C Composites with Excellent Electromagnetic Wave Absorption Properties. *ACS Appl. Mater. Interfaces,* 2015, **7**, 13604–13611.
11. Li, N.; Hu, C. W.; Cao, M. H. Enhanced Microwave Absorbing Performance of CoNi Alloy Nanoparticles Anchored on a Spherical Carbon Monolith. *Phys. Chem. Chem. Phys.,* 2013*,* **15***,* 7685–7689.
12. Li, X. A.; Zhang, B.; Ju, C. H.; Han, X. J.; Du, Y. C.; Xu, P. Morphology-Controlled Synthesis and Electromagnetic Properties of Porous $Fe_3O_4$ Nanostructures from Iron Alkoxide Precursors. *J. Phys. Chem. C,* 2011, **115***,* 12350–12357.